Nonadiabatic collisions of CaH with Li: Importance of spin-orbit-induced spin relaxation in spin-polarized sympathetic cooling of CaH

Mick Warehime*
Chemical Physics Program, University of Maryland, College Park, Maryland 20742, USA

Jacek Kłos†
Department of Chemistry and Biochemistry, University of Maryland, College Park, Maryland 20742, USA
(Received 27 May 2015; revised manuscript received 27 July 2015; published 8 September 2015)

We apply our recently developed, quantum, nonadiabatic, two-dimensional finite element method [Warehime *et al.*, J. Chem. Phys. **142**, 034108 (2015).] to estimate the probability of the nonadiabatic reaction in spin-polarized $Li(^2S) + CaH(^2\Sigma^+)$. This spin-orbit-induced reaction leads to trap loss due to the opening of a barrierless pathway to the $Ca(^1S) + LiH(^1\Sigma^+)$ products. To investigate this reaction we calculate three two-dimensional radial cuts of the potential energy surfaces for the triplet and singlet electronic states. We also calculate the spin-orbit coupling matrix element between these two electronic states. From our nonadiabatic scattering calculations we estimate the spin-flip probability in the sympathetic cooling of the CaH molecule with ultracold Li atoms to be small: on the order of 10^{-7} and increasing to 10^{-4} at higher temperatures. We estimate the order of the rate constant in our reduced dimensionality approach for the reaction proceeding on the singlet potential at a temperature of 1 K to be 10^{-10} cm^3/s. This is of the same order as the measured value of 3.6×10^{-10} cm^3/s [Singh *et al.*, Phys. Rev. Lett. **108**, 203201 (2012)]. This reaction rate is at least seven orders of magnitude larger than our estimated rate of the spin-orbit-induced triplet to singlet reaction. Our nonadiabatic result is encouraging for the experimental prospects for this title system.

DOI: 10.1103/PhysRevA.92.032703 PACS number(s): 34.50.Cx, 34.50.Lf, 95.30.Ft

I. INTRODUCTION

There is recently much interest to efficiently produce cold and ultracold molecules [1–3]. The field of low-temperature chemistry offers increased control over the quantum state of the reactants and collision energy resolution. The cold regime also allows for precise single-molecule spectroscopy [4] and control over chemical reactions using external fields or trapping cold molecules in optical lattices [5] and magnetic traps [6]. Optical lattices are a promising tool for realizations of quantum information objectives, i.e., quantum computers and simulators [7].

The magnetic trapping and cotrapping of cold atoms and molecules are tools for precise studies of collision dynamics and measurements that can reveal new physics [8]. Stark deceleration has been used successfully to slow down supersonic beams of polar molecules such as OH [9,10] and ND_3 [11]. Sub-kelvin reactions have also been studied by exploiting the Zeeman effect. In such reactions curved magnetic quadrupole guides are used to merge a beam of molecules with a magnetic moment, such as metastable rare-gas atoms, with another beam of molecules to investigate resonances in the ultracold reaction regime [12–15].

Reaction kinetics in the low kelvin regime have also been studied by the so-called CRESU technique [16]. Sims and coworkers [17] have recently used this technique to determine the $F+H_2$ reaction rate from 11 K to 295 K. These measurements, which are well below the 800 K reaction barrier, confirmed that the reaction rate in the low-temperature regime is driven by quantum tunneling effects.

Beams of slow moving molecules can also be used as a source for loading molecular traps. A slow beam of $CaH(X\,^2\Sigma^+)$ molecules has been realized by the two-stage cell buffer gas method [18,19]. A similar method has been used to prepare a source of slow CaF molecules [6]. In the present study we are interested in the feasibility of using these techniques to cool CaH molecules to sub-kelvin temperatures via controlled interactions with a beam of ultracold Li atoms.

The plausibility of using ultracold Li atoms for sympathetic cooling of CaH molecules in a spin-polarized state has been demonstrated in scattering calculations [20]. The calculations on the spin-polarized Li-CaH triplet surface show a favorable ratio of elastic to inelastic collisions, which predicts minimal collision induced losses. Tscherbul *et al.* claim that extending the CaH interatomic distance does not lead to the reaction on the triplet surface. However, nonadiabatic transitions from the triplet to singlet surface may lead to the following exothermic reaction:

$$Li(^2S) + CaH(^2\Sigma^+) \rightarrow Ca(^1S) + LiH(^1\Sigma^+). \quad (1)$$

The exothermicity of this reaction calculated from the experimental dissociation energy of LiH [21] and experimentally derived dissociation energy of CaH [22] is 0.750 eV.

Low-temperature collisions on the endothermic triplet surface are not reactive due to the high energy of the excited products. The spin-orbit coupling between triplet and singlet surfaces, however, may lead to depolarizing the high spin state in either the reactive or nonreactive channels. Recently, Tscherbul and Buchachenko [23] estimated the rate constant for reaction on the singlet surface using the adiabatic channel capture theory, and their results are in good agreement with experiment at 1 K [19].

*mickwarehime@gmail.com
†Corresponding author: jklos@umd.edu

However, the question of whether the spin-relaxing pathways in the spin-orbit coupled triplet-singlet system will induce significant losses of trapped CaH remains open. To this end we present reduced dimensionality finite element method (2D-FEM) studies of reactive and nonreactive collisions between Li and CaH on the triplet ($S = 1$) potential-energy surface which is coupled by the spin-orbit term to the barrierless singlet ($S = 0$) surface. We first calculate new potential surfaces for the singlet and triplet states as well as the spin-orbit coupling term from first-principle configuration interaction calculations.

This paper is organized as follows. In Sec. II we describe the computational methodology employed in the *ab initio* calculations of the potential-energy surfaces. Section III presents the scattering calculations methodology and their results and discussion. The paper's conclusions are presented in Sec. IV.

II. *AB INITIO* POTENTIAL SURFACES

In this study we are interested in the interaction between Li(^2S) atom and the CaH molecule in the ground electronic $X\,^2\Sigma^+$ state. In our *ab initio* approach to calculate the $S = 0$ (singlet), and spin-polarized $S = 1$ (triplet) potential-energy surfaces and the spin-orbit coupling between these surfaces we used the state-averaged complete active space configurational self-consistent field (SA-CASSCF) method [24,25] to obtain reference orbitals for subsequent internally contracted multireference configuration interaction calculations including explicitly single and double excitations (*ic*-MRCISD) [26,27]. The Langhoff and Davidson [28] correction was applied to account for effects of higher excitations in an approximate manner. The Ca atom was described by an all-electron correlation consistent quadruple-zeta basis set (cc-pvQZ) of Koput *et al.* [29] and the Li atom by an augmented, correlation consistent quadruple-zeta basis set (aug-cc-pVQZ) and hydrogen by the aug-cc-pVTZ basis set of Dunning [30].

The reference wave function for the CASSCF calculations were obtained from the restricted Hartree-Fock calculations (RHF) for the high-spin case. The first step of the CASSCF calculations was to perform state-averaged calculations for the singlet and triplet states. The active space in the CASSCF calculation was composed of 13 orbitals in A' representation and three orbitals of A'' representation of the C_s symmetry group. The first four A' and one A'' orbitals were kept frozen with an additional four A' orbitals and one correlated A'' orbital kept doubly occupied.

Using the MRCI density matrices for the $S = 0$ and $S = 1$ Li-H-Ca electronic states we calculated spin-orbit coupling [31] matrix elements between the two surfaces. The potentials and spin-orbit matrix element were calculated for geometry described by two bond coordinates, u_{LiH} and u_{HCa}, and $\angle$ Li-H-Ca bond angle θ. We calculated the potential surfaces

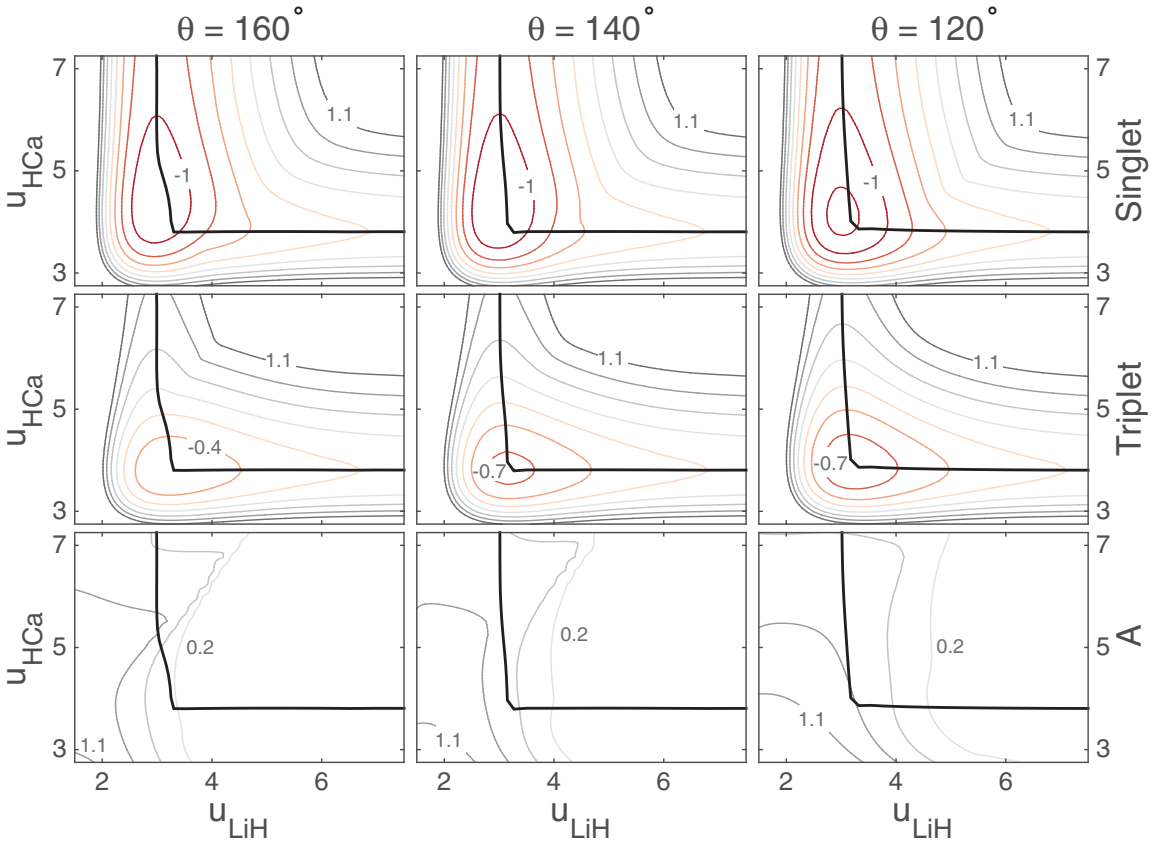

FIG. 1. (Color online) Potential contours of the Li+CaH reaction for the singlet surface in eV (top), triplet surface in eV (middle), and spin-orbit matrix element in meV (bottom) as a function of bond coordinates in bohr. The contour lines are evenly spaced at intervals of 0.3 eV and 0.3 meV for the singlet, triplet and spin-orbit surfaces, respectively. The thick black line corresponds to the minimum energy path (from Weinan's method [32]) for a given angle.

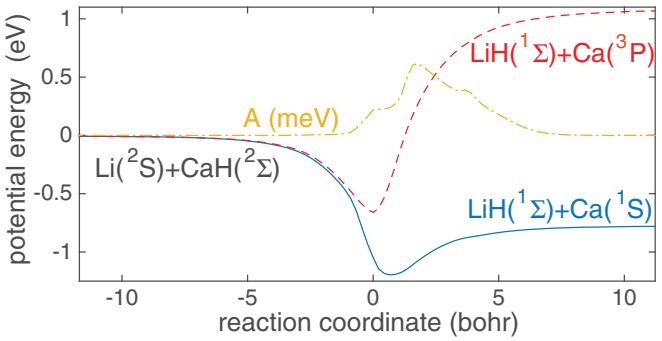

FIG. 2. (Color online) Potential curves of the Li+CaH reaction for the singlet (blue solid line) and triplet (red dashed line) states in eV and spin-orbit coupling matrix element A (yellow dash-dotted line) in meV along the minimum energy path for $\theta = 160^\circ$ (from Weinan's method [32]). The reaction coordinate is measured from the minimum of the triplet surface.

and the coupling term for the θ bond angles of 160°, 140°, and 120° and on a grid of interatomic distance from 1.4 to $24a_0$ for u_{LiH} and from 1.8 to $24a_0$ for u_{HCa}. We choose these specific bond angles as they are corresponding to the vicinity of the global minimum on the triplet energy surface, as we are mainly interested in the approach on the triplet surface and resulting spin-flip to a singlet manifold.

Figure 1 shows the contour plots of the potential energy surfaces and spin-orbit constant in the interaction region for each fixed value of θ. In Fig. 2 we show the potential-energy surfaces along the minimum energy path along the triplet surface for $\theta = 160$. Lastly, we provide the descriptive parameters of each potential surface in Table I. The triplet minima have values close to the one calculated by Tscherbul *et al.* [20], where they find the global minimum $V_{\min}$ of the Li-CaH triplet potential to be −0.88 eV for the CaH distance fixed at the equilibrium geometry and for the Li-H distance of $3.33a_0$. In the present calculations the electronic energy of the Ca+LiH products lies 0.779 eV below the energy of the Li+CaH reactants. Our calculated exothermicity on the singlet surface is 0.766 eV. This correlates well with the exothermicity of 0.750 eV mentioned earlier for reaction (1) from the experimentally derived values [21,22]. We note that the exothermicity for the reaction (1) given by Tscherbul *et al.* [20] is slightly different, where they give the value of 0.67 eV. The difference may be explained by using somewhat different dissociation energy values. We believe our value of the exothermicity should be more exact.

TABLE I. Minimum geometries for the singlet and triplet surfaces of Li+CaH. Values given in degrees, bohr, and eV.

	θ	u_{LiH}	u_{HCa}	$V_{\min}$
Singlet	120	2.99	4.19	−1.37
	140	2.99	4.23	−1.27
	160	2.99	4.40	−1.24
Triplet	120	3.19	3.90	−0.91
	140	3.19	3.82	−0.78
	160	3.22	3.82	−0.66

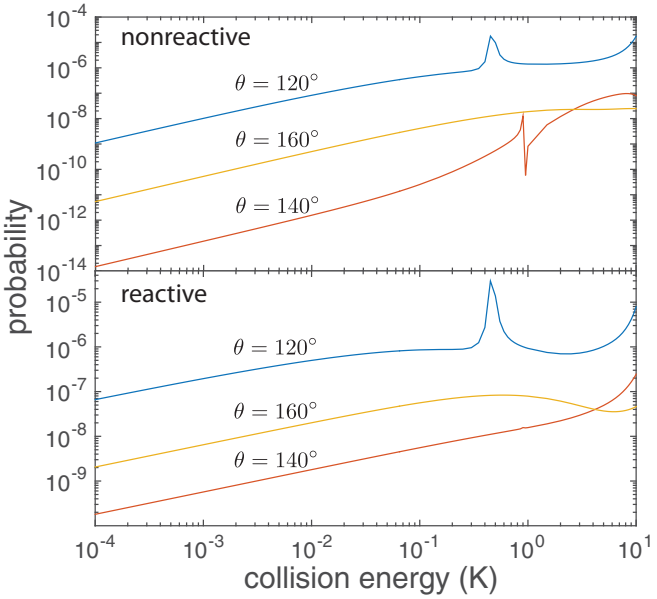

FIG. 3. (Color online) Top panel: spin-orbit-induced spin-relaxing (triplet → singlet) $Li(^2S) + CaH(^2\Sigma, v = 0) \rightarrow Li(^2S) + CaH(^2\Sigma, v' = \text{all})$, nonreactive scattering probabilities summed over all final v' states. Bottom panel: spin-orbit-induced reactive scattering probabilities summed over all final states for triplet → singlet $Li(^2S) + CaH(^2\Sigma, v = 0) \rightarrow Ca(^1S) + LiH(^1\Sigma, v' = \text{all})$. Probabilities are given for each of the three bond angles.

III. SCATTERING CALCULATIONS

We use our finite-element (F.E.) based reactive scattering package [33,34] to simulate the nonadiabatic reaction dynamics of the Li+CaH system evolving on the coupled singlet and triplet potential surfaces. Our reduced dimensional F.E. code solves the time-independent formulation of Schrödinger's equation for collinear, reactive atom-diatom collisions with coupled potential surfaces, which allows for nonadiabatic transitions. The scattering package uses mass-scaled Jacobi coordinates and simultaneously solves for the reactive scattering wave function and all reactive and nonreactive S-matrix elements. The computational details of our F.E. scattering package have been described elsewhere [33,34].

In the present work we are interested in the probability of spin-orbit-induced nonadiabatic transitions between the singlet and triplet surfaces of Li+CaH. The singlet and triplet surfaces are coupled by the spin-orbit operator $A(Q)$, namely,

$$\mathbf{V}(Q) = \mathbf{V}_{el}(Q) + \mathbf{V}_{\text{SO}}(Q) = \begin{bmatrix} V_{S=0}(Q) & 0 \\ 0 & V_{S=1}(Q) \end{bmatrix} + \begin{bmatrix} 0 & A(Q) \\ A(Q) & 0 \end{bmatrix}, \tag{2}$$

where Q refers, collectively, to the bond coordinates.

In Fig. 3 we provide the results of the scattering simulations at low collision energies for nonreactive (top panel) and reactive (bottom panel) collisions, respectively. In these scattering calculations we use the mass of the most abundant isotope for each atomic species, namely, ^{7}Li, ^{1}H, and ^{40}Ca. We have also calculated the singlet → singlet reactive probabilities in this range of collision energies. Though not pictured here the

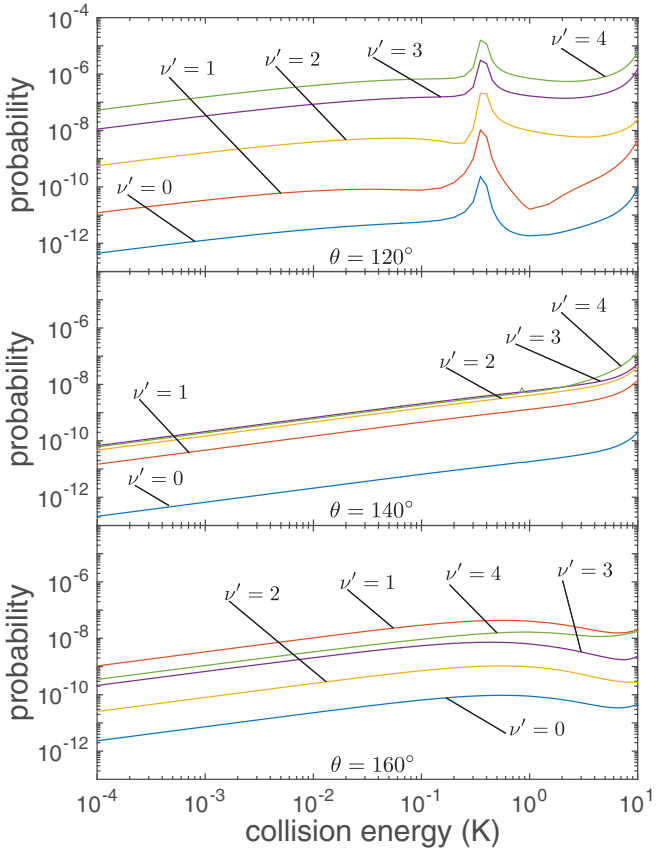

FIG. 4. (Color online) Vibrational state-to-state, spin-orbit-induced reactive scattering probabilities for triplet → singlet $\mathrm{Li}(^2S) + \mathrm{CaH}(^2\Sigma, v = 0) \rightarrow \mathrm{Ca}(^1S) + \mathrm{LiH}(^1\Sigma, v')$ as a function of a bond angle.

spin-orbit-induced singlet → singlet reaction probabilities are on average seven orders of magnitude larger than the triplet → singlet probabilities. The resonancelike structure appearing in probabilities at 1 K in Fig. 3 is likely a resonance in the exit channel or a resonance with the opening of a vibrational state. The analysis of such resonances is out of the scope of this paper having in mind our approximate reduced-dimensionality approach.

One expects the full three-dimensional scattering calculations to vary from these results qualitatively. Based on our results, however, it is unlikely that the inclusion of rotational dynamics would increase the nonadiabatic transition probability by several orders of magnitude. Accordingly, we are confident that the spin-orbit-induced nonadiabatic transitions will not be a significant pathway to trap loss in the Li+CaH system.

Figure 4 shows the vibrational specificity of the spin-orbit-induced, nonadiabatic reactive scattering probabilities. In every case the LiH products are vibrationally hot. It is interesting to note the distinct anisotropy with respect to the vibrational specificity of the LiH products as a function of collision angle.

We have also determined the orders of rate constants for the triplet to singlet and singlet to singlet reactions $\mathrm{Li}(^2S)+\mathrm{CaH}(^2\Sigma, v = 0) \rightarrow \mathrm{LiH}(^1\Sigma, v') + \mathrm{Ca}(^1S)$ using the

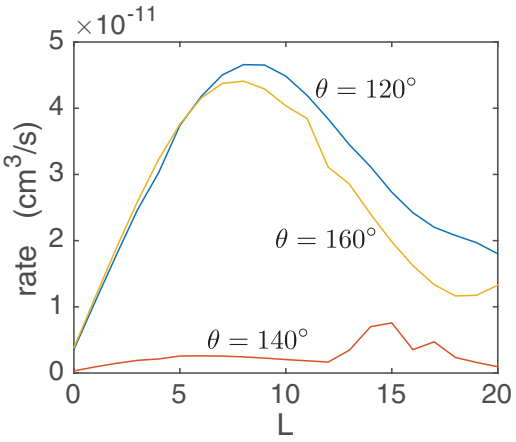

FIG. 5. (Color online) Cumulative rate constant for $T = 1$ K as a function of angular orbital momentum quantum number L for the singlet → singlet $\mathrm{Li}(^2S) + \mathrm{CaH}(^2\Sigma, v = 0) \rightarrow \mathrm{Ca}(^1S) + \mathrm{LiH}(^1\Sigma, v' = \text{all})$ reaction as a function of a bond angle.

usual expression

$$k_{v\rightarrow v'}(T) = \left(\frac{8}{\mu\pi(k_bT)^3}\right)^{1/2} \int_0^\infty \sigma_{v\rightarrow v'} e^{-E/(k_bT)} E\, dE,$$

where μ is the reduced mass of the system in the reactant arrangement and v and v' are the initial and final vibrational states of the diatomics, and E is a collision energy. We estimate the order of the singlet to singlet reaction rate to be 10^{-10} cm^3/s. Singh *et al.* [19] have recently measured the singlet reaction rate to be 3.6×10^{-10} cm^3/s at $T = 1$ K with a factor of 2 of uncertainty. Tscherbul and Buchachenko [23] have recently calculated the Li+CaH reaction rate to be 7.1×10^{-10} cm^3/s using the adiabatic channel capture theory using only triplet long-range CCSD(T) potential [20]. Although we cannot directly compare our results using the reduced dimensionality model with experiment or the three-dimensional theory, we emphasize our prediction of the triplet to singlet reaction rate to be seven orders of magnitude smaller than our predictions of the singlet to singlet reaction rate.

To approximate the effects of end-over-end rotation we have included a diagonal centrifugal $\frac{\hbar^2 L(L+1)}{2\mu R^2}$ term to the potential. We then determined the reaction rate as a function of the angular momentum quantum number, L, and the total reaction rate was the sum over all values of L up to the maximum value $L_{\max} = 21$. This L dependence of the reaction rate is shown in Fig. 5. Depending on the angle, the maximum contributions are for $L = 7$–9, similar to $L = 6$–7 contributions by Tscherbul *et al.* [23] and we confirm that most of the significant contributions to the rate at 1 K are from $L \leqslant 20$ ($L \leqslant 18$ by Tscherbul *et al.* [23]).

IV. CONCLUSIONS

Nonadiabatic transitions are most probable when the off-diagonal elements of the coupling potential are on the order of magnitude of the difference between the diagonal potential surfaces. Based on the new *ab initio* potential surfaces presented in this work, we have found that the

spin-orbit coupling never satisfies this requirement. Our scattering calculations, albeit in reduced dimensionality, have shown that for collision energies relevant in ultracold cooling methods, the spin-orbit-induced triplet-singlet transitions are negligibly small (seven or more orders of magnitude smaller) compared to the singlet-singlet transitions. Our estimated order of the rate constant for the singlet to singlet Li+CaH reaction is the same as the rate order from previous theoretical estimation and experimental measurement at 1 K. Our results embolden the claim made by Tscherbul and co-workers [20] that lithium atoms are promising collision partners to produce ultracold CaH molecules.

ACKNOWLEDGMENTS

We would like to thank Professor Millard Alexander for many discussions and encouragement in this project. We are grateful for the financial support from the National Science Foundation (Grant No. CHE-1213332) to M. H. Alexander.

[1] *Cold Molecules: Theory, Experiment, Applications*, edited by R. Krems, W. C. Stwalley, and B. Friedrich (CRC Press; Taylor & Francis Group, Boca Raton, FL, 2009).
[2] D. Patterson, J. Rasmussen, and J. M. Doyle, New J. Phys. **11**, 055018 (2009).
[3] D. S. Jin and J. Ye, Chem. Rev. **112**, 4801 (2012).
[4] H. Loh, K. C. Cossel, M. C. Grau, K.-K. Ni, E. R. Meyer, J. L. Bohn, J. Ye, and E. A. Cornell, Science **342**, 1220 (2013).
[5] M. H. G. de Miranda, A. Chotia, B. Neyenhuis, D. Wang, G. Quéméner, S. Ospelkaus, J. L. Bohn, J. Ye, and D. S. Jin, Nat. Phys. **7**, 502 (2011).
[6] H.-I. Lu, I. Kozyryev, B. Hemmerling, J. Piskorski, and J. M. Doyle, Phys. Rev. Lett. **112**, 113006 (2014).
[7] R. V. K. Lincoln, D. Carr, D. DeMille, and J. Ye, New J. Phys. **11**, 055049 (2009).
[8] J. J. Hudson, D. M. Kara, I. J. Smallman, B. E. Sauer, M. R. Tarbutt, and E. A. Hinds, Nature (London) **473**, 493 (2011).
[9] S. Y. T. van de Meerakker, P. H. M. Smeets, N. Vanhaecke, R. T. Jongma, and G. Meijer, Phys. Rev. Lett. **94**, 023004 (2005).
[10] M. Kirste, L. Scharfenberg, J. Kłos, F. Lique, M. H. Alexander, G. Meijer, and S. Y. T. van de Meerakker, Phys. Rev. A **82**, 042717 (2010).
[11] H. L. Bethlem, F. M. H. Crompvoets, R. T. Jongma, S. Y. T. van de Meerakker, and G. Meijer, Phys. Rev. A **65**, 053416 (2002).
[12] A. Henson, S. Gersten, Y. Shagam, J. Narevicius, and E. Narevicius, Science **338**, 234 (2012).
[13] E. Lavert-Ofir, Y. Shagam, A. B. Henson, S. Gersten, J. Kłos, P. S. Żuchowski, J. Narevicius, and E. Narevicius, Nat. Chem. **6**, 332 (2014).
[14] J. Jankunas, B. Bertsche, K. Jachymski, M. Hapka, and A. Osterwalder, J. Chem. Phys. **140**, 244302 (2014).
[15] J. Jankunas, K. Jachymski, M. Hapka, and A. Osterwalder, J. Chem. Phys **142**, 164305 (2015).
[16] I. R. Sims and I. W. M. Smith, Annu. Rev. Phys. Chem. **46**, 109 (1995).
[17] M. Tizniti, S. D. L. Picard, F. Lique, C. Berteloite, A. Canosa, M. H. Alexander, and I. R. Sims, Nat. Chem. **6**, 141 (2014).
[18] H.-I. Lu, J. Rasmussen, M. J. Wright, D. Patterson, and J. M. Doyle, Phys. Chem. Chem. Phys. **13**, 18986 (2011).
[19] V. Singh, K. S. Hardman, N. Tariq, M.-J. Lu, A. Ellis, M. J. Morrison, and J. D. Weinstein, Phys. Rev. Lett. **108**, 203201 (2012).
[20] T. V. Tscherbul, J. Kłos, and A. A. Buchachenko, Phys. Rev. A **84**, 040701 (2011).
[21] W. C. Stwalley and W. T. Zemke, J. Phys. Chem. Ref. Data **22**, 87 (1993).
[22] T. V. R. Rao, J. Mol. Struct. (Theochem) **105**, 249 (1983).
[23] V. Tscherbul and A. A. Buchachenko, New J. Phys. **17**, 035010 (2015).
[24] H.-J. Werner and P. J. Knowles, J. Chem. Phys. **82**, 5053 (1985).
[25] P. J. Knowles and H.-J. Werner, Chem. Phys. Lett. **115**, 259 (1985).
[26] H.-J. Werner and P. J. Knowles, J. Chem. Phys. **89**, 5803 (1988).
[27] P. J. Knowles and H.-J. Werner, Theor. Chim. Acta **84**, 95 (1992).
[28] S. R. Langhoff and E. R. Davidson, Int. J. Quantum Chem. **8**, 61 (1974).
[29] J. Koput and K. A. Peterson, J. Phys. Chem. A **106**, 9595 (2002).
[30] T. H. Dunning, J. Chem. Phys. **90**, 1007 (1989).
[31] A. Berning, M. Schweizer, H.-J. Werner, P. J. Knowles, and P. Palmieri, Mol. Phys. **98**, 1823 (2000).
[32] E. Weinan, R. Weiqing, and E. Vanden-Eijnden, J. Chem. Phys. **126**, 164103 (2007).
[33] M. Warehime and M. H. Alexander, J. Chem. Phys **141**, 024118 (2014).
[34] M. Warehime, J. Kłos, and M. H. Alexander, J. Chem. Phys. **142**, 034108 (2015).